

# Advances in Materials Science for Environmental and Nuclear Technology II

*Edited by*  
S. K. Sundaram  
Tatsuki Ohji  
Kevin Fox  
Elizabeth Hoffman

**Ceramic**  
**T**ransactions  
Volume 227

 **WILEY**



This page intentionally left blank

---

# Advances in Materials Science for Environmental and Nuclear Technology II

---

---

This page intentionally left blank

# Advances in Materials Science for Environmental and Nuclear Technology II

---

Ceramic Transactions, Volume 227

Edited by  
S. K. Sundaram  
Kevin Fox  
Tatsuki Ohji  
Elizabeth Hoffman



A John Wiley & Sons, Inc., Publication

Copyright © 2011 by The American Ceramic Society. All rights reserved.

Published by John Wiley & Sons, Inc., Hoboken, New Jersey.

Published simultaneously in Canada.

No part of this publication may be reproduced, stored in a retrieval system, or transmitted in any form or by any means, electronic, mechanical, photocopying, recording, scanning, or otherwise, except as permitted under Section 107 or 108 of the 1976 United States Copyright Act, without either the prior written permission of the Publisher, or authorization through payment of the appropriate per-copy fee to the Copyright Clearance Center, Inc., 222 Rosewood Drive, Danvers, MA 01923, (978) 750-8400, fax (978) 750-4470, or on the web at [www.copyright.com](http://www.copyright.com). Requests to the Publisher for permission should be addressed to the Permissions Department, John Wiley & Sons, Inc., 111 River Street, Hoboken, NJ 07030, (201) 748-6011, fax (201) 748-6008, or online at <http://www.wiley.com/go/permission>.

**Limit of Liability/Disclaimer of Warranty:** While the publisher and author have used their best efforts in preparing this book, they make no representations or warranties with respect to the accuracy or completeness of the contents of this book and specifically disclaim any implied warranties of merchantability or fitness for a particular purpose. No warranty may be created or extended by sales representatives or written sales materials. The advice and strategies contained herein may not be suitable for your situation. You should consult with a professional where appropriate. Neither the publisher nor author shall be liable for any loss of profit or any other commercial damages, including but not limited to special, incidental, consequential, or other damages.

For general information on our other products and services or for technical support, please contact our Customer Care Department within the United States at (800) 762-2974, outside the United States at (317) 572-3993 or fax (317) 572-4002.

Wiley also publishes its books in a variety of electronic formats. Some content that appears in print may not be available in electronic formats. For more information about Wiley products, visit our web site at [www.wiley.com](http://www.wiley.com).

*Library of Congress Cataloging-in-Publication Data is available.*

ISBN: 978-1-118-06000-1

ISBN: 1042-1122

oBook ISBN: 978-1-118-14452-7

ePDF ISBN: 978-1-118-14449-7

Printed in the United States of America.

10 9 8 7 6 5 4 3 2 1

---

# Contents

---

Preface	ix
---------	----

## **CLEAN ENERGY: MATERIALS, PROCESSING, AND MANUFACTURING**

Slag Characterization for the Development of New and Improved Service Life Materials in Gasifiers using Flexible Carbon Feedstock James Bennett, Seetharaman Sridhar, Jinichiro Nakano, Kyei-Sing Kwong, Tom Lam, Tetsuya Kaneko, Laura Fernandez, Piyamanee Komolwit, Hugh Thomas, and Rick Krabbe	3
Characterization of Electrochemical Cycling Induced Graphite Electrode Damage in Lithium-Ion Cells Sandeep Bhattacharya, A. Reza Riahi, and Ahmet T. Alpas	17
Titanium-Dioxide-Coated Silica Microspheres for High-Efficiency Dye-Sensitized Solar Cell Devender and Ajay Dangi	27
Effect of Titanium and Iron Additions on the Transport Properties of Manganese Cobalt Spinel Oxide Jeffrey W. Fergus, Kangli Wang, and Yingjia Liu	33
Effect of Hydrogen on Bending Fatigue Life for Materials used in Hydrogen Containment Systems Patrick Ferro	39

Investigation of Secondary Phases Formation Due to $\text{PH}_3$ Interaction with SOFC Anode Huang Guo, Gulfam Iqbal, and Bruce Kang	51
PEN Structure Thermal Stress Analysis for Planar-SOFC Configurations under Practical Temperature Field Gulfam Iqbal, Suryanarayana Raju Pakalapati, Francisco Elizalde-Blancas, Huang Guo, Ismail Celik, and Bruce Kang	61
Electroless Coating of Nickel on Electrospun 8YSZ Nanofibers Luping Li, Peigen Zhang, and S.M. Guo	69
Effect of Surface Condition on Spallation Behavior of Oxide Scale on SS 441 Substrate used in SOFC Wenning Liu, Xin Sun, Elizabeth Stephens, and Moe Khaleel	81
Effect of Fuel Impurity on Structural Integrity of Ni-YSZ Anode of SOFCs Wenning Liu, Xin Sun, Olga Marina, Larry Pederson, and Moe Khaleel	87
Strategies to Improve the Reliability of Anode-Supported Solid Oxide Fuel Cells with Respect to Anode Reoxidation Manuel Ettler, Norbert H. Menzler, Georg Mauer, Frank Tietz, Hans Peter Buchkremer, and Detlev Stöver	101
Mixed Composite Membranes for Low Temperature Fuel Cell Applications Uma Thanganathan	111
Carbonate Fuel Cell Materials and Endurance Results C. Yuh, A. Hilmi, G. Xu, L. Chen, A. Franco, and M. Farooque	119

## **MATERIALS SOLUTIONS FOR THE NUCLEAR RENAISSANCE**

Characterization of Core Sample Collected from the Saltstone Disposal Facility A.D. Cozzi and A.J. Duncan	135
Incorporation of Mono Sodium Titanate and Crystalline Silicotitanate Feeds in High Level Nuclear Waste Glass K. M. Fox, F. C. Johnson, and T. B. Edwards	149
Radiation Resistance of Nanocrystalline Silicon Carbide Laura Jamison, Peng Xu, Kumar Sridharan, and Todd Allen	161
Performance of a Carbon Steel Container in a Canadian Used Nuclear Fuel Deep Geological Repository Gloria M. Kwong, Steve Wang, and Roger C. Newman	169



Development of Ceramic Waste Forms for an Advanced Nuclear Fuel Cycle	183
A. L. Billings, K. S. Brinkman, K. M. Fox and J. C. Marra, M. Tang, and K. E. Sickafus	
Determination of Stokes Shape Factor for Single Particles and Agglomerates	195
J. Matyáš, M. Schaible, and J. D. Vienna	
Glassy and Glass Composite Nuclear Wasteforms	203
Michael I. Ojovan and William E. Lee	
Advances in Materials Corrosion Research in the Yucca Mountain Project	217
Raul B. Rebak	
Creep Studies of Modified 9Cr-1Mo Steel for Very High Temperature Reactor Pressure Vessel Applications	231
Triratna Shrestha, Mehdi Basirat, Indrajit Charit, Gabriel Potirniche, and Karl Rink	
Developing the Plutonium Disposition Option: Ceramic Processing Concerns	241
Jonathan Squire, Ewan R. Maddrell, Neil C Hyatt, and Martin C. Stennett	
Pore Structure Analysis of Nuclear Graphites IG-110 and NBG-18	251
G. Q. Zheng, P. Xu, K. Sridharan, and T. R. Allen	

## **GREEN TECHNOLOGIES FOR MATERIALS MANUFACTURING AND PROCESSING**

Modified Powder Processing as a Green Method for Ferrite Synthesis	263
Audrey Vecoven and Allen W. Apblett	
Novel Method for Waste Analysis using a Highly Luminescent (II) Octaphosphite Complex as a Heavy Metal Detector	279
Nisa T. Satumtira, Ali Mahdy, Mohamed Chehbouni, Oussama ElBjeirami, and Mohammad A. Omary	
Geopolymer Products from Jordan for Sustainability of the Environment	289
Hani Khoury, Yousif Abu Salhah, Islam Al Dabsheh, Faten Slaty, Mazen Alshaaer, Hubert Rahier, Muayad Esaifan, and Jan Wastiels	
Leaching of Calcium Ion (Ca <sup>2+</sup> ) from Calcium Silicate	301
Vandana Mehrotra	

Green Energy and Green Materials Production Activity and Related Patents	313
J. A. Sekhar, M. C. Connelly, and J. D. Dismukes	
Micro Patterning of Dielectric Materials by using Stereo-Lithography as Green Process	329
Soshu Kiriara, Naoki Komori, Toshiki Niki, and Masaru Kaneko	
Author Index	337

---

# Preface

---

The Materials Science and Technology 2010 Conference and Exhibition (MS&T'10) was held October 17-21, 2010, in Houston, Texas. A major theme of the conference was Environmental and Energy Issues. Papers from three of the symposia held under that theme are included in this volume. These symposia include Clean Energy: Fuel Cells, Batteries, Renewables – Materials, Processing and Manufacturing; Materials Solutions for the Nuclear Renaissance; and Green Technologies for Materials Manufacturing and Processing. These symposia included a variety of presentations with sessions focused on Advanced Nuclear Fuels, Materials Performance in Extreme Environments, Immobilization of Nuclear Wastes, Irradiation and Corrosion Effects, Modeling, Solid Oxide Fuel Cells, Batteries, Clean Fuel Combustion, and Solar Energy.

The success of these symposia and the publication of the proceedings could not have been possible without the support of The American Ceramic Society and the organizers of the above mentioned symposia. The symposia organizers included William E. Lee, Josef Matyas, Ramana G. Reddy, Kumar Sridharan, Zhenguo (Gary) Yang, Prabhakar Singh, Prashant Kumta, Ayyakkannu Manivannan, Abdul-Majeed Azad, Colleen Legzdins, Arumugam Manthiram, Donald W. Collins, Mri-tyunjay Singh, Richard Sisson, and Allen Apblett. Their assistance, along with that of the session chairs, was invaluable in ensuring the creation of this volume.

S. K. SUNDARAM, *Alfred University, USA*

KEVIN FOX, *Savannah River National Laboratory, USA*

TATSUKI OHJI, *AIST, JAPAN*

ELIZABETH HOFFMAN, *Savannah River National Laboratory, USA*

This page intentionally left blank

# Clean Energy: Materials, Processing, and Manufacturing

---

This page intentionally left blank

## SLAG CHARACTERIZATION FOR THE DEVELOPMENT OF NEW AND IMPROVED SERVICE LIFE MATERIALS IN GASIFIERS USING FLEXIBLE CARBON FEEDSTOCK

James Bennett<sup>1</sup>, Seetharaman Sridhar<sup>1,2</sup>, Jinichiro Nakano<sup>1</sup>, Kyei-Sing Kwong<sup>1</sup>, Tom Lam<sup>1,3</sup>, Tetsuya Kaneko<sup>1,2</sup>, Laura Fernandez<sup>1,2</sup>, Piyamanee Komolwit<sup>1,2</sup>, Hugh Thomas<sup>1</sup>, Rick Krabbe<sup>1</sup>

<sup>1</sup> US Department of Energy National Energy Technology Laboratory, 1450 Queen Ave., Albany, OR 97321 USA

<sup>2</sup> Department of Materials Science and Engineering, Carnegie Mellon University, 5000 Forbes Ave., Pittsburgh, PA 15213 USA

<sup>3</sup> Alfred University, 1 Saxon Dr., Alfred, NY 14802 USA

### ABSTRACT

In modern gasifiers, the carbon feedstock (coal, petcoke and/or biomass) is determined largely by carbon content, cost, availability, and environmental concerns. Ash impurities in the carbon feedstock vary widely in quantity and chemistry, impacting gasifier operation. Ash from mineral impurities in the feedstock liquefy at the elevated temperatures of gasification; impacting slag chemistry, viscosity, melting temperature, surface and interfacial tension – ultimately determining gasifier operating temperature and refractory service life. The slag itself experiences wide variations in the relative fraction and state of crystalline material (oxides, sulfides and metallic), non-crystalline (glass) material, or gas phases formed from feedstock ash. It is these variations that have a critical impact gasifier operation, determining slag fluidity along the walls and the chemical and physical stability (wear) of the refractory liner. In this paper, two aspects of joint research between NETL and CMU on slag and slag/refractory interactions will be discussed. The first area is researching phase formation in synthetic petcoke/coal slag ( $\text{SiO}_2\text{-Al}_2\text{O}_3\text{-Fe}_2\text{O}_3\text{-CaO-V}_2\text{O}_5$ ) under simulated gasification conditions (1500°C and  $10^{-8}$  atm oxygen partial pressure). The second area focuses on interactions between coal and petcoke slags with commercial refractory currently used (high chrome oxide) or having the potential for use as a gasifier liner (high alumina). Refractory materials studied in the simulated gasifier environment were fired brick of the following compositions: 90wt% $\text{Cr}_2\text{O}_3\text{-10wt}\%\text{Al}_2\text{O}_3$  and 100wt% $\text{Al}_2\text{O}_3$ . Information from this research is being used to improve the performance of or to develop new refractory liner materials for gasifiers, and to understand mixed feedstock slag behavior under gasification conditions.

### INTRODUCTION

Gasification as a modern industrial process converts carbon feedstock (typically coal and petcoke), water, and oxygen (oxygen shortage - reducing concentration) at elevated temperatures and high pressure into CO and  $\text{H}_2$ ; with excess heat, gases (typically  $\text{CO}_2$ ,  $\text{H}_2\text{S}$ ,  $\text{CH}_4$ ,  $\text{NH}_3$ , HCN,  $\text{N}_2$ , and Ar), slag (from mineral impurities in the carbon feedstock), and carbon (excess added to ensure maximum CO production) produced as process by-products. The CO/ $\text{H}_2$  (syngas) product from a gasifier is used for power generation, as a feedstock for the chemical industry (used in the production of chemicals including fertilizer or Fischer Tropsch liquids), and is considered a leading candidate for  $\text{H}_2$  production in a hydrogen based economy. Gasification is being explored as a critical technology in the success of DOE's Near Zero Emissions Advanced Fossil Fuel Power Plants, and could play a key role in defining the nation's long-term energy security in both power and liquid fuels. With a DOE goal of 90 pct  $\text{CO}_2$  capture, the closed loop

of high pressure gasification is easily adapted to supply a “pure” CO<sub>2</sub> stream for reuse or sequestration, giving it a cost advantage over many other processes. It thought that if biomass is used as a part of a carbon feedstock in gasification, approximately 30 pct of the total carbon additions as biomass will make the process carbon neutral.

Several types of gasifiers exist, with this research focused on the entrained bed air cooled slagging gasifier, which produces a molten slag from mineral impurities in the carbon feedstock. These gasifiers, shown in figure 1, are lined with high chrome oxide refractory materials that lasts anywhere from 3 months to 30 months, a life determined by operating conditions and the severity of the gasifier environment. The operating conditions of slagging gasifiers involves temperatures between 1325°-1575°C, a reducing atmosphere (about 10<sup>-8</sup> oxygen partial pressure), and pressures between 2.07 – 6.89 MPa. In that environment, the service life of the high chrome oxide liner does not meet the performance needs of gasifier users, and limits achieving an on line gasifier availability of 85-95% targeted for utility applications and more than 95% in applications such as chemical feedstock production<sup>1</sup>. Failure to meet these goals has created a potential roadblock to widespread acceptance and commercialization of advanced gasification technology, and is the reason refractory liners were identified as a key barrier to widespread commercialization of gasification technology<sup>2</sup>.

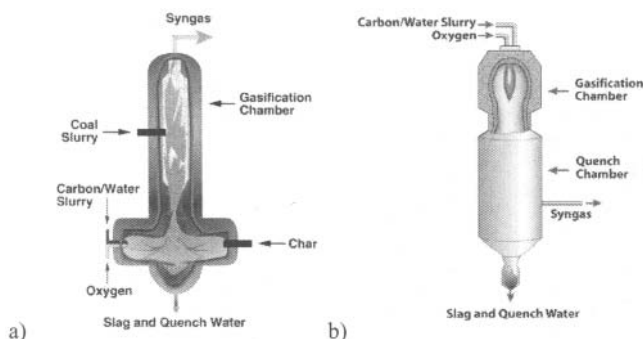


Figure 1. Two types of slagging gasifiers used by industry; a) two stage slagging gasifier, and b) single stage gasifier.

Failure of the hot face gasifier lining is expensive, both in terms of material replacement costs (as high as \$1,000,000) and in lost production (due to the 1-3 week gasifier shutdown for liner repair/replacement and the resulting lost syngas production). Besides current performance issues, questions also exist concerning high chrome oxide linings and fuel flexibility. High alkali and alkaline earth levels found in new carbon sources being considered for gasification, such as biomass or western coals, will change refractory liner wear and may cause the formation of hexavalent chrome oxide in the refractory liner; resulting in their possible classification as a hazardous waste. Non-chrome oxide materials, which were evaluated for their potential as a gasifier liner material in the mid 70's through the mid 80's by USDOE, EPRI, and industry sponsored research, were found to have inferior performance when compared to high chrome oxide refractories<sup>3-8</sup>. Chrome oxide levels above 75 pct have been determined to survive the severe service environment of gasification<sup>9</sup>. Current additives to chrome oxide that contribute to



their superior corrosion performance are alumina and zirconia. Since the early research, improvements in raw material purity, grain structure, and in refractory fabrication technology have occurred that merit non-chrome oxide materials to be re-evaluated as gasifier containment materials, especially with regard to mixed feedstock environments. The practice of mixed feedstock will make it highly unlikely that any one brick composition will have adequate performance in all slag environments – the impact of potential slag compositions must be evaluated and used to determine liner materials. Additional benefits of no or low chrome oxide refractories could include lower cost (due to the use of raw materials with lower cost than chrome oxide), lower brick density (leading to lighter brick weight per unit size), an increased number of refractory material suppliers (creating an environment for increased innovation and price competition), and faster installation of linings (non-chrome oxide materials have the potential for installation techniques not possible with high chrome oxide liner materials).

Carbon feedstock currently used in slagging gasifiers includes coal, petroleum coke, or combinations of them. Because of the rising cost of carbon feedstock, concerns over CO<sub>2</sub> emissions, feedstock availability, as well as other drivers; fuel flexibility (the use of mixed or varying carbon feedstock in gasification) is currently practiced or considered by many gasifier operators. One drawback to fuel flexibility is the unknown effect impurities present in them have on the liner service life and the gasification process. Mineral impurities in carbon feedstock can range up to 10 wt pct or higher for coal, 1 wt pct for petcoke, and from 1 to 20 wt pct for biomass. The impurities of concern include oxides of Si, Al, Ca, Mg, Fe, K, Na, and V; which may form aggressive molten slags at the high temperature of gasification, slags that dissolve or penetrate the refractory liner and lead to their premature failure. Besides gasifier temperature, oxygen partial pressure, and the quantity of ash associated with the carbon feedstock will also impact liner wear. In addition to lining wear, slag must flow from a gasifier. Additives to control slag flow and the temperature of gasification may be made, but have an unknown impact on refractory wear. Past refractory research focused on developing highly slag resistant refractory materials, but failed to consider other properties of slags from carbon feedstock, and how modification of them might reduce refractory wear and impart good slag flow properties. Slag chemistry can be controlled to minimize interactions with the refractory liner or its penetration into the porous refractory. Known wear mechanisms of refractories caused by slag include structural spalling (brought about by slag penetration into a refractory), chemical spalling (caused by slag/refractory interactions on the refractory surface), and/or corrosion (chemical dissolution of the refractory in the slag)<sup>10</sup>. Instead of considering slag impact on lining wear, the gasifier is typically operated at a temperature where slag will flow it as a liquid, yet will produce the desired syngas composition. If a gasifier is operated at too low of a temperature, slag will not flow from it, instead clogging the exit and leading to premature system shutdown. If the gasifier is operated at too high a temperature, accelerated wear of the refractory lining will occur, a known consequence that is not controlled.

To obtain a fundamental understanding of the interactions of mixed carbon feedstock with current and proposed refractory liner materials, the National Energy Technology Laboratory (NETL) and Carnegie Mellon University (CMU) have partnered to evaluate slag phases formed under gasification conditions and to study the slag/refractory interactions of those mixed feedstock materials. This paper summarizes the joint research that has been conducted.

## COAL AND PETCOKE SLAG CHEMISTRY

A range of coal ash chemical compositions exist in the U.S.; with gasifier use dependent on the price, carbon content, availability, shipping distance, ash and moisture content, and other factors. Petcoke used in gasification also vary greatly in ash chemistry; with its feedstock use dependent on factors similar to coal. Because of the wide variations in coal chemistry, an average based on approximately 300 analyses<sup>11</sup> was used as a base for compositions in this research, and an average of nine for petcoke<sup>12-14</sup>. Those chemistries are listed in table 1; with Al, Si, Fe, Ca, and V the most critical for slag viscosity and refractory/slag interactions. Oxides of these compounds have a large impact on slag viscosity, refractory dissolution, and the ability of slag to wet and penetrate refractory surfaces; properties which influence refractory wear.

Of the coal and petcoke ashes generated in a slagging gasifier, the behavior of petcoke slag under gasification conditions is the least understood; with limited thermodynamic data available on vanadium in software program (such as FactSage™) at low oxygen partial pressures and elevated temperatures encountered during gasification. Because of the lack of this fundamental information, slag behavior and materials interactions of mixed feedstock are difficult to predict, and are the focus of reported research. Mixed feedstock containing biomass will be evaluated at a later date, with elements of concern in biomass including Al, Si, Fe, Ca, K, Mg, and Na.

Table 1. Average coal<sup>11</sup> and petcoke<sup>12-14</sup> slag compositions used to evaluate mixed feedstock slag properties.

Ash Source	Percent Ash	Wt Pct Oxide								
		Al <sub>2</sub> O <sub>3</sub>	SiO <sub>2</sub>	Fe <sub>2</sub> O <sub>3</sub>	CaO	MgO	Na <sub>2</sub> O	K <sub>2</sub> O	V <sub>2</sub> O <sub>5</sub>	NiO
Avg. Coal	10.0	27.0	46.6	16.4	6.2	1.3	1.0	1.5	NA	NA
Avg. Petcoke	1.0	5.4	16.0	7.4	6.1	1.1	0.9	0.6	53.1	9.5

NA = Not analyzed

## KINETIC STUDIES OF SYNTHETIC COAL/PETCOKE CRYSTAL FORMATION

### Research Objective/Test Description

The study of coal/petcoke mixture crystallization under gasification conditions is discussed below, which was previously reported<sup>15</sup>. A total of six average coal and petcoke mixtures (based on the chemical compositions in table 1) were ball milled in 500 ml Nalgene® plastic bottles containing ethanol as a grinding/mixing procedure for 48 hours using reagent grade oxide powders (starting particle size below 44 microns). The chemistry of the mixed slags was analyzed by ICP, with the results given in table 2. A Confocal Scanning Laser Microscope (CSLM – Lasertec ILM21H) was used to melt samples, with a figure of the furnace and sample holder assembly shown in figure 2. Slag samples were placed in a cylindrical platinum crucible (99.99 pct Pt) prior to the melting and quenching experiment. Mixtures were heated in air to 1500°C at rate of 77°C/sec and “premelting” to produce liquid slag, after which the furnace was cooled to a specific test temperature, held for 2 minutes, then the furnace environment changed to a CO/CO<sub>2</sub> gas mixture to create an oxygen partial pressure of 10<sup>-8</sup> atm – similar to that existing in a commercial gasifier at that temperature. Initial heating was done in air because thermodynamic data did not exist on V<sub>2</sub>O<sub>5</sub> liquid formation at 1500°C, while the starting vanadium compound of V<sub>2</sub>O<sub>5</sub> was known to completely liquefy in air. After samples were held at the desired test temperature for 2 minutes, a CO/CO<sub>2</sub> gas mixture was introduced to create an

oxygen partial pressure of approximately  $10^{-8}$  atm and the time for initial crystallization to occur on the slag surface recorded. When the atmosphere was changed from air to CO/CO<sub>2</sub> (creating an O<sub>2</sub> partial pressure of approximately  $10^{-8}$ ), vanadium oxide present in the mixture shifted in composition to V<sub>2</sub>O<sub>3</sub>, and crystallization of supersaturated vanadium solutions occurred.

Table 2. Chemistry of petcoke/coal slag mixtures used in time temperature transformation studies.

Petcoke/Coal Ash Wt Ratio	Oxide Chemistry (wt pct)					
	SiO <sub>2</sub>	Al <sub>2</sub> O <sub>3</sub>	CaO	Fe <sub>2</sub> O <sub>3</sub>	K <sub>2</sub> O	V <sub>2</sub> O
0/100	52.0	24.0	6.4	14.5	2.9	0
10/90	49.3	22.4	6.8	14.1	2.7	4.7
30/70	43.9	19.2	7.5	13.2	2.4	13.7
50/50	38.4	15.9	8.3	12.3	2.0	23.1
70/30	32.9	12.6	9.0	11.5	1.7	32.5
100/0	25.0	7.8	10.1	10.2	1.2	46.0

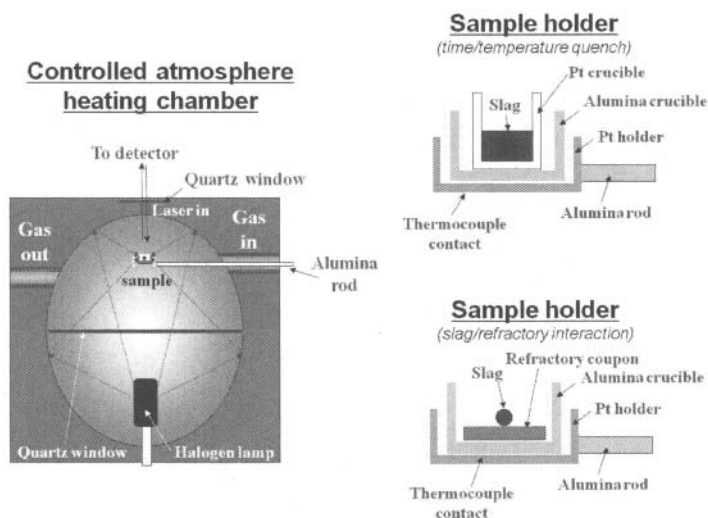


Figure 2 Confocal Scanning Laser Microscope used for heating test samples of slag in Pt crucibles or slag on refractory coupons. Slag and refractory materials are shown in the sample chamber.

## Results and Conclusions

The crystallization sequence at different times for a petcoke slag at 1500°C is shown in figure 3. Note that crystallization of V<sub>2</sub>O<sub>3</sub> did not occur until about 50 seconds after the atmosphere change. The crystallization in figure 3 occurred at the pre-melting temperature of the slag mixture in air, and indicated the impact oxygen partial pressure has on the phases of vanadium present in the liquid slag.

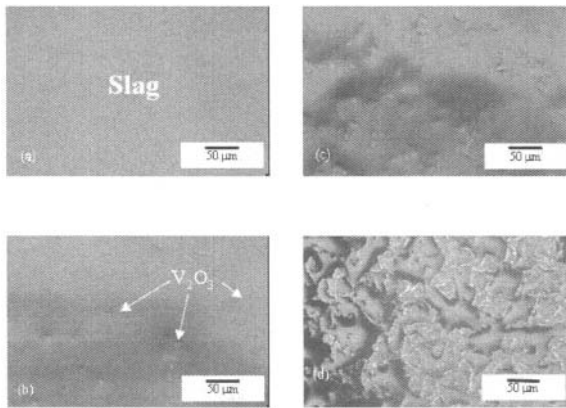


Figure 3. Crystallization sequence for a 100 pct petcoke mixture at 1500°C and an oxygen partial pressure of  $10^{-8}$  atm. Times to crystallization in the images are as follows: a) 47 sec; b) 52 sec; c) 60 sec; and d) 138 sec. Images b, c, and d show the crystallization of  $V_2O_3$  (karelianite).

Crystallization as a time temperature transformation diagram occurring at an oxygen partial pressure of  $10^{-8}$  atm is shown in figure 4. At temperatures above 1500°C, karelianite ( $V_2O_3$ ) was the primary phase identified. At lower temperatures tested (below about 1350°C), phases of karelianite, spinels ( $VFe_2O_4$ ,  $FeV_2O_4$ , and  $FeAl_2O_4$ ), and anorthorite ( $CaO \cdot Al_2O_3 \cdot 2SiO_2$ ) were found to precipitate. Slag compositions containing 10 wt pct or less petcoke did not have any phases that precipitated above about 1375°C, while compositions containing 100 wt pct petcoke had no phases other than karelianite that precipitated. Above 1350°C, only karelianite was found to precipitate in all compositions. It is of interest that a thermodynamic program, FactSage™, suggested mullite may also be stable at temperatures above 1350°C, a phase not found in these rapid quench studies, but a phase identified in long term coal/petcoke phase equilibrium studies presented in the next section.

Phases that precipitated from a slag influence overall system viscosity, remaining liquid viscosity (because of chemistry changes in the liquid), the ability of the altered liquid slag to penetrate pores, and how the liquid slag interacts with the refractory. As mentioned, greater detail of the study is found in the original work<sup>15</sup>.

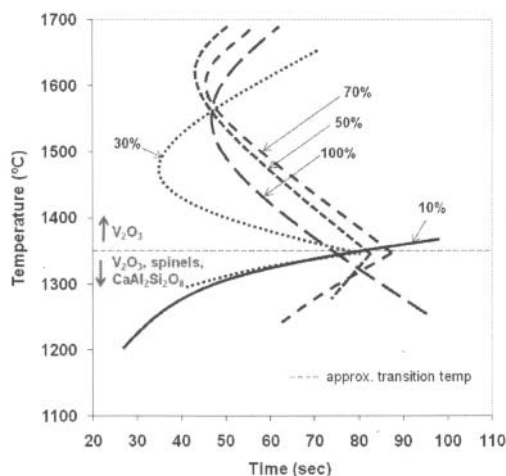


Figure 4. Time temperature transformation diagram showing crystallization of different petcoke/coal mixtures at an oxygen partial pressure of  $10^{-8}$  atm.

#### THERMODYNAMIC STUDIES OF PHASE EQUILIBRIA IN SYNTHETIC COAL/PETCOKE MIXED SLAGS

##### Research Objective/Test Description

The phase equilibrium of synthetic coal/petcoke mixtures composed of five oxide components ( $\text{SiO}_2$ - $\text{Al}_2\text{O}_3$ - $\text{FeO}$ - $\text{CaO}$ - $\text{V}_2\text{O}_3$ ) were studied as part of an effort to establish phase equilibrium conditions to use in thermodynamic databases. This work is on-going, and the research presented represents preliminary data. The five oxides considered in this study are the major components in coal and petcoke slags impacting viscosity and wear behavior. Phase information obtained from the study will be used to predict equilibrium conditions existing in gasifiers. The average coal and petcoke compositions used in the study are listed in table 3, and have their origin in the petcoke and compositions listed in table 1. The ratios of petcoke and coal evaluated corresponded to petcoke to coal additions of 0-72 pct on a carbon feedstock basis. Because the amount of  $\text{V}_2\text{O}_3$  increases as petcoke additions were made and the amount of  $\text{FeO}$  and  $\text{CaO}$  stayed fairly constant,  $\text{FeO}$  and  $\text{CaO}$  were fixed at constant values in the study, while  $\text{SiO}_2$ ,  $\text{Al}_2\text{O}_3$ , and  $\text{V}_2\text{O}_3$  were varied, with ratios of  $\text{Al}_2\text{O}_3$  and  $\text{SiO}_2$  ranging from 1/4 to 1/1.

Exposure conditions for the petcoke/coal compositions were  $1500^\circ\text{C}$  at an oxygen partial pressure of  $10^{-8}$  atm (obtained by using a 64%  $\text{CO}$ /36%  $\text{CO}_2$  gas exposure environment). Samples were held at temperature for 72 hours to obtain equilibrium. Oxides used in the study were reagent grade materials with particle sizes less than 44 microns. Powders were dry mixed in 150 ml Nalgene<sup>®</sup> plastic bottles at 55 rpm, with mixing stopped and manual stirring done on a periodic basis to prevent agglomerates from forming and to improve mixing. A total of 450 mgs of each mixed powder was placed individually in Pt crucibles (99.99 pct pure) that were approximately 10mm diameter and 7.5 mm high. The Pt crucibles containing test material was then placed in an alumina trays for handling and quenching (as shown in figure 5). Test

materials was heated to 1200°C at a rate of 191°C/hr, followed by a heating rate of 120°C/hr to 1500°C. After the timed sample soak at 1500°C, samples were quenched in water to “freeze” phases present, after which they were analyzed for crystalline phases and chemistry using XRD (Rigaku Ultima III), SEM (JEOL-7000F), and TEM (Phillips CM200).

Table 3. Chemistry and phases formed in petcoke/coal compositions after a 72 hr exposure at 1500°C in a 10<sup>-8</sup> atm oxygen partial pressure.

Sample	Chemical Composition (Wt Pct)					Phase Identified
	Al <sub>2</sub> O <sub>3</sub>	CaO	FeO	SiO <sub>2</sub>	V <sub>2</sub> O <sub>5</sub>	
1	14.7	6.9	12.8	65.6	0	Slag
2	18.8	6.9	12.8	61.4	0	Slag
3	14.7	6.7	12.8	64.2	1.7	Slag
4	36.5	6.6	15.8	41	0	Slag + Mullite
5	25.1	6.6	12.7	55.7	0	Slag + Mullite
6	38.9	7	13.5	39	1.6	Slag + Mullite
7	35.4	7	14.3	39.8	3.5	Slag + Mullite
8	33.6	7.5	14	38.9	6	Slag + Mullite
9	32.8	6.9	13.7	44.4	2.1	Slag + Mullite
10	11.7	6.4	12.3	60.9	8.7	Slag + Karelitanite
11	20.8	6.6	15.9	49.6	7	Slag + Karelitanite
12	14.2	6.8	14	62	3	Slag + Karelitanite
13	15	7	12.1	60.9	4.9	Slag + Karelitanite
14	33.9	7.7	13.8	36.6	8	Slag + Karelitanite + Mullite
15	25.1	6.9	14.2	46.4	7.4	Slag + Karelitanite +Mullite
16	28.7	7.6	13.1	42.8	7.7	Slag + Karelitanite + Mullite

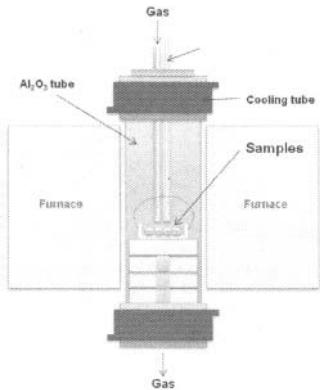


Figure 5. Furnace and experimental setup used to expose synthetic petcoke/coal slag samples at 1500°C to an oxygen partial pressure of 10<sup>-8</sup> atm.

## Results and Conclusions

The following phases were noted in the petcoke/coal slag composition listed in table 3: amorphous slag, mullite ( $3\text{Al}_2\text{O}_3 \cdot 2\text{SiO}_2$ ), and karelianite ( $\text{V}_2\text{O}_3$ ). Some substitution of vanadium for aluminum in the mullite structure, and of aluminum for vanadium in the karelianite structure was noted, and is being evaluated further. A preliminary isothermal phase diagram based on the data obtained to date is shown in figure 6, along with SEM images of the phases formed at  $1500^\circ\text{C}$ . Phase equilibrium data is being obtained for under other temperatures and oxygen partial pressures conditions, and will be used to revise this proposed phase diagram.

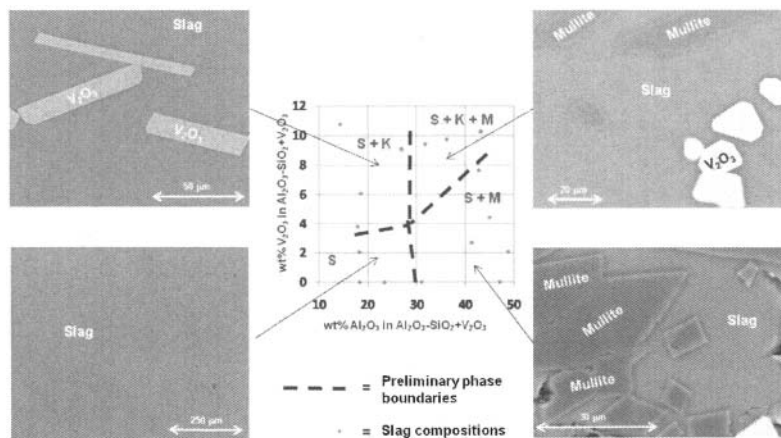


Figure 6. Preliminary equilibrium phase diagram versus chemistry of petcoke/slag synthetic mixtures with 13.5 wt pct FeO and 7 wt pct CaO and variations of  $\text{SiO}_2$ ,  $\text{Al}_2\text{O}_3$ , and  $\text{V}_2\text{O}_3$  when they were exposed to a simulated gasifier environment of  $1500^\circ\text{C}$ , and oxygen partial pressure of  $10^{-8}$  atm. Phases are S = Slag, K = Karelitanite, M = Mullite

Four phase areas are included in the proposed isothermal phase diagram (figure 6) and include slag, slag plus mullite, slag plus karelianite, and slag plus mullite and karelianite. Typical coal/petcoke carbon feedstock and the corresponding slags formed from them should fall within the proposed diagram; and indicate system saturation and changes in mullite with respect to changes in  $\text{Al}_2\text{O}_3$  and  $\text{SiO}_2$ . Slags high in petcoke may become saturated with  $\text{V}_2\text{O}_3$  or  $\text{V}_2\text{O}_5$  and mullite, depending on the amount of  $\text{Al}_2\text{O}_3$  and vanadium present and the system temperature and oxygen partial pressure.

## INTERACTIONS OF REFRACTORY MATERIALS ( $\text{Al}_2\text{O}_3$ and $\text{Cr}_2\text{O}_3$ ) WITH COAL AND PETCOKE SLAGS

### Research Objective/Test Description

Interactions between coal and petcoke slags and refractory materials currently used (high chrome oxide) or with potential for use as gasifier liner materials (high alumina in this study) were previously evaluated<sup>16</sup> to understand interface reactions occurring at the surface and are

summarized in this section. Synthetic coal and petcoke slag compositions were used, with the compositions listed in table 4. Note that both petcoke and coal slag compositions are based on compositions previously described and listed in table 1. Two refractory materials were evaluated, a high chrome oxide commercial material of approximate composition 90 wt pct  $\text{Cr}_2\text{O}_3$ /10 wt pct  $\text{Al}_2\text{O}_3$ ; and a silica bonded high alumina commercial refractory that was 99 pct  $\text{Al}_2\text{O}_3$ . Chemical and physical properties of the refractory materials are also listed in table 4.

Table 4. Chemical and physical properties of synthetic slag (petcoke and coal) and refractory compositions used to evaluate interface interactions.

	Slag		Refractory Material*	
	Petcoke	Coal	High Chrome	High Alumina
<b>Chemistry (wt %)</b>				
- $\text{SiO}_2$	25	52	0.2	0.2
- $\text{Al}_2\text{O}_3$	7.8	24	10.2	99.6
- $\text{CaO}$	10.1	6.4	0.3	Trace
- $\text{MgO}$	NA	NA	0.1	Trace
- $\text{Fe}_2\text{O}_3$	10.2	14.5	0.1	0.1
- $\text{K}_2\text{O}$	1.2	2.9	NA	NA
- $\text{Na}_2\text{O} + \text{K}_2\text{O}$	-	-	NA	0.1
- $\text{V}_2\text{O}_5$	46	NA	-	-
- $\text{Cr}_2\text{O}_3$	-	-	89.0	NA
- $\text{TiO}_2$	-	-	0.2	Trace
<b>Apparent Porosity (%)</b>	-	-	16.7	19.4

NA = Not analyzed

\* = Data from product data sheet

Synthetic slag mixtures listed in table 4 were pre-melted in carbon crucibles by heating above their melting temperature in high purity Ar for two hours. Slag samples then were reheated a second time for 2 hours at 1500°C in an atmosphere of CO/CO<sub>2</sub> to create stable phases existing in that environment prior to testing. Coal or petcoke slags particles were then placed on specific test coupon areas (grains or matrix) for timed exposures at 1500°C of 0 or 10 minutes. Reactions of the premelted slag on the refractory coupon were evaluated as sessile drop interactions using the CSLM described earlier and shown in figure 2. The heating rate for samples tested was approximately 77°C/sec to the test temperature of 1500°C. Slag particles were approximately 300-500 microns in diameter and weighed between 0.02 and 0.04 mg. Refractory coupons were approximate 3 mm square by 1 mm thick, with a surface finish of 1 micron. Testing was done in a CO/CO<sub>2</sub> atmosphere corresponding to an oxygen partial pressure of 10<sup>-8</sup> atm. After heating and holding at 1500°C for the designated time, test samples were He quenched at an average cooling rate from 99°C/sec from 1500 to 900°C, then cooled at 77°C/sec to room temperature. Exposed surface and side profile microstructures were evaluated by SEM to determine changes occurring at the slag/refractory interaction. A total of 16 experiments were conducted.

## Results and Conclusions

Slag and high chrome, high alumina refractory surface microstructures (after 10 minutes of exposure at 1500°C in a CO/CO<sub>2</sub> atmosphere corresponding to an oxygen partial pressure of 10<sup>-8</sup> atm) are shown in figures 7 and 8 respectively. Significant surface changes were not noted on either the coal or petcoke slags that contacted high chrome grains, although when petcoke



contacted grains of high chrome oxide, it wet and spread; and it appeared to wet and interact with grains of alumina, with crystallization of  $V_2O_5$  occurring on the surface of alumina grains.

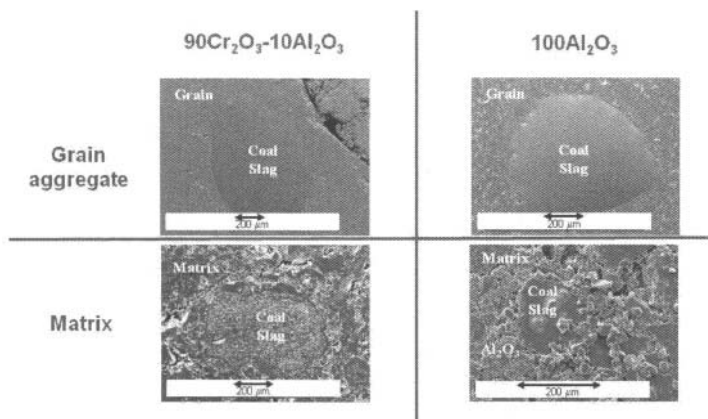


Figure 7. Surface interactions between coal slag and commercial refractory samples (high chrome oxide and alumina) after 10 minutes of exposure at 1500°C in a CO/CO<sub>2</sub> atmosphere corresponding to an oxygen partial pressure of  $10^{-8}$  atm.

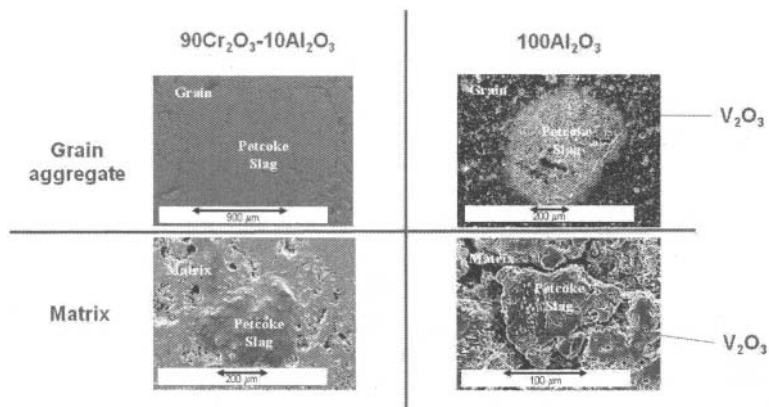


Figure 8. Surface interactions between petcoke slag and commercial refractory samples (high chrome oxide and alumina) after 10 minutes of exposure at 1500°C in a CO/CO<sub>2</sub> atmosphere corresponding to an oxygen partial pressure of  $10^{-8}$  atm.

When interactions between coal and petcoke slags and the high chrome and alumina matrix materials were evaluated, coal slag wet and penetrated the high chrome oxide matrix, while the high alumina matrix interacted with the slag and had high alumina grains that were released from the contact area, remaining on the surface of the coupon (figure 7). Petcoke slags penetrated the surface of the high chrome oxide refractory, and had excess slag containing

particles (figure 8). When the petcoke slag interacted with the high alumina material, a coarser surface resulted, probably from material dissolution into the slag and the release of some alumina grains.

The greater interaction of petcoke slags with high alumina materials would indicate the potential for greater refractory wear during service and thus, a shorter service life. The potential for greater wear in high chrome oxide refractory materials was also indicated when exposed to petcoke slags. A cross section image of petcoke slag/high chrome oxide matrix material exposed for 10 minutes (figure 9) showed possible chemical spalling of a Cr/V compound at the slag/refractory interface. This type wear mechanism is known to occur in high chrome oxide refractories exposed to coal slag [17].

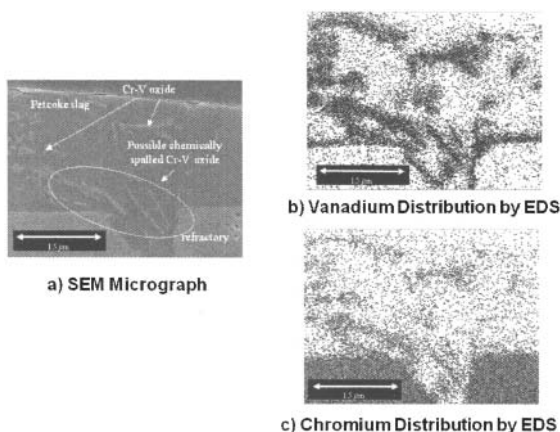


Figure 9. Cross section of petcoke slag/high chrome oxide refractory interface evaluated by SEM after 10 minutes of exposure at 1500°C in a CO/CO<sub>2</sub> atmosphere corresponding to an oxygen partial pressure of 10<sup>-8</sup> atm. a) slag/refractory cross section, b) EDS imaging indicating vanadium, and c) EDS imaging for chrome. Note the possible chemical spalling on the surface of Cr/V compound.

## CONCLUSIONS

Gasification is used to produce CO and H<sub>2</sub> (syngas), with two types of feedstock (coal and petcoke) used individually or in mixtures as carbon sources. Syngas generated by gasification is used in the production of power and chemicals, and is a possible source of H<sub>2</sub> in a hydrogen based economy. Gasification as an industrial process is limited by the on line availability of the process, which is directly impacted by refractory liner failure. Mineral impurities in the carbon feedstock create ash; which at the high temperature (1325-1575°C) and low oxygen partial pressures (10<sup>-8</sup> atm) of gasification, melt to produce molten slag. The molten slag interacts with the Cr<sub>2</sub>O<sub>3</sub> refractory liner currently used to protect the gasifier, causing refractory failure primarily by chemical corrosion or spalling. The properties of slag can be controlled to reduce refractory wear or to develop improved performance refractory materials, but are not well understood. NETL and CMU have conducted joint research using synthetic

coal/petcoke slags to study: 1) slag properties under gasification conditions, and 2) slag/refractory interactions. The following conclusions concerning slags and refractory/slag interactions under gasification conditions can be drawn:

- Synthetic coal/petcoke slags containing  $\text{SiO}_2\text{-Al}_2\text{O}_3\text{-FeO-CaO-V}_2\text{O}_5$  were heated to  $1500^\circ\text{C}$  in a Confocal Scanning Laser Microscope (CSLM), then cooled at different temperatures for up to 2 minutes. Karelitanite ( $\text{V}_2\text{O}_5$ ) was formed as the primary phase above  $1350^\circ\text{C}$ ; and karelitanite, spinels ( $\text{VFe}_2\text{O}_4$ ,  $\text{FeV}_2\text{O}_4$ , and  $\text{FeAl}_2\text{O}_4$ ), and anorthite ( $\text{CaO-Al}_2\text{O}_3\text{-2SiO}_2$ ) were formed below  $1350^\circ\text{C}$ . Synthetic slag containing 100 pct petcoke formed only karelitanite at all test temperatures. Synthetic slag containing 0 and 10 pct petcoke formed no phase other than slag above  $1375^\circ\text{C}$ .
- Different synthetic coal/petcoke slag compositions containing  $\text{SiO}_2\text{-Al}_2\text{O}_3\text{-FeO-CaO-V}_2\text{O}_5$  were heated at  $1500^\circ\text{C}$  for 72 hrs in an oxygen partial pressure of  $10^{-8}$  atm. Based on phase formation four regions are proposed in a preliminary phase diagram: slag; slag plus karelitanite; slag plus mullite ( $3\text{Al}_2\text{O}_3\text{-2SiO}_2$ ); or slag, mullite and karelitanite. The type of phases formed was dependent on slag composition.
- Interactions between mixtures of synthetic coal/petcoke slags and commercial high chrome and alumina refractories evaluated at  $1500^\circ\text{C}$  for 10 minutes in an oxygen partial pressure of  $10^{-8}$  atm using a CSLM indicated the greatest interactions between coal and petcoke slags and alumina refractory materials. Chemical spalling was noted on high chrome oxide refractories and petcoke slags.

Knowledge of the properties of coal and petcoke slags under gasification conditions is being used to develop improved performance refractory materials, or to improve the performance of existing gasifier materials through the possible control of slag properties.

## REFERENCES

- <sup>1</sup> G. Stiegel, and S. Clayton, "DOE Gasification Industry R& D Survey: A Perspective of Long Term Market Trends and R&D Needs"; Proceedings of the Gasification Technologies 2001 Annual Meeting; San Francisco, CA.
- <sup>2</sup> Gasification Markets and Technologies – Present and Future – An Industry Perspective; US DOE/FE Report 0447; US DOE; (July, 2002); pp. 1-53.
- <sup>3</sup> J.A. Bonar, C.R. Kennedy, and R.B. Swaroop; "Coal-Ash Slag Attack and Corrosion of Refractories"; Amer. Ceram. Soc. Bul.; Vol. 59, No. 4, 1980; pp 473-478.
- <sup>4</sup> W.T. Bakker, Greenberg, M. Trondt, and U. Gerhardus; "Refractory Practice in Slagging Gasifiers"; Amer. Ceram. Soc. Bul.; Vol. 63, No. 7, 1984; pp 870-876.
- <sup>5</sup> S. Greenberg and R.B. Poeppel, "The Corrosion of Ceramic Refractories Exposed to Synthetic Coal Slags by Means of the Rotation-Cylinder Technique: Final Report," Research Report ANL/FE—85-15, research sponsored by USDOE/FE and EPRI, April 1986, 66 pp.
- <sup>6</sup> A.P. Starzacher, "Picrochromite Brick - A Qualified Material for Texaco Slagging Gasifiers," Radex-Rundschau, Vol. 1, 1988, pp. 491-501.
- <sup>7</sup> R.E. Dial, "Refractories for Coal Gasification and Liquefaction," Amer. Ceram. Soc. Bul., Vol. 54, No. 7 (1975), pp 640-43.
- <sup>8</sup> M.S. Crowley, "Refractory Problems in Coal Gasification Reactors," Amer. Ceram. Soc. Bul.; Vol. 54, No. 12 (1975), pp 1072-74.
- <sup>9</sup> W.T. Bakker, "Refractories for Present and Future Electric Power Plants," Key Engineering

Materials, Trans Tech Publications, (1993), Vol. 88, pp. 41-70.

<sup>10</sup> J.P. Bennett, J. Kwong, B. Riggs (Eastman Chemical, Kingsport, TN); Identification and Elimination of Refractory Failure in an Air Cooled Slagging Gasifier; Proceedings of the 44th Annual Ref. Sym.; St. Louis, MO; March 26-27, 2008.

<sup>11</sup> W.A. Selvig and F.H. Gibson; "Analysis of Ash from United States Coals"; USBM Bulletin, Pub. 567; 1956; 33 pp.

<sup>12</sup> S.V. Vassilev et al; "Low Cost Catalytic Sorbents for NO<sub>x</sub> Reduction. 1. Preparation and Characterization of Coal Char Impregnated with Model Vanadium Components and Petroleum Coke Ash"; Fuel; Vol 81, 2002; pp 1281-1296.

<sup>13</sup> R.E. Conn; "Laboratory Techniques for Evaluating Ash Agglomeration Potential in Petroleum Coke Fired Circulating Fluidized Bed Combustors"; Fuel Pro.Tech.; Vol 44, 1995; pp 95-103.

<sup>14</sup> R.W. Bryers; "Utilization of Petroleum Coke and Petroleum Coke/Coal Blends as a Means of Steam Raising"; Fuel Proc. Tech.; Vol. 44, 1995; pp 121-141.

<sup>15</sup> J. Nakano, S. Sridhar, T. Moss, J. Bennett, and K.S. Kwong; "Crystallization of Synthetic Coal-Petcoke Slag Mixtures Simulating Those Encountered in Entrained Bed Slagging Gasifiers"; Energy and Fuels; 23, 2009; pp 4723-4733.

<sup>16</sup> J. Nakano, S. Sridhar, J. Bennett, K.S. Kwong, and T. Moss; "Interactions of Refractory Materials With Molten Gasifier Slags"; Inter. J. of Hydrogen Energy ; 2010; doi:10.1016/j.ijhydene.2010.04.117.

<sup>17</sup> J.P. Bennett, K.S. Kwong, H. Thomas, and R. Krabbe; "Post-Mortem Analysis of High Chrome Oxide Refractory Liners from Slagging Gasifiers Using Analytical Tools/Thermodynamics"; presented and published in CD proceedings of UNITECR 2009; Oct, 2009; Salvador, Brazil; 4 pp.

## CHARACTERIZATION OF ELECTROCHEMICAL CYCLING INDUCED GRAPHITE ELECTRODE DAMAGE IN LITHIUM-ION CELLS

Sandeep Bhattacharya, A. Reza Riahi, Ahmet T. Alpas  
Department of Mechanical, Automotive and Materials Engineering  
University of Windsor, 401 Sunset Avenue,  
Windsor, Ontario, Canada N9B 3P4

### ABSTRACT

Electrodes made of high purity graphite were subjected to electrochemical tests to investigate graphite surface degradation using in-situ observations by means of a digital microscope with large depth of field. The fraction of graphite removed from the surface increased with decreasing voltage scan rate. Cross-sectional SEM investigations of samples prepared using focused ion-beam (FIB) milling indicated that SEI deposits were formed preferentially inside the cavities on graphite surface. Subsurface damage features of graphite included partial delamination of the graphite layers and fragmentation of graphite into fine particles.

### INTRODUCTION

The high reversible lithium capacity (372 mAh/g) as well as good electronic and ionic conductivity of graphite has made it the preferred anode material for rechargeable lithium-ion batteries<sup>1</sup>. However, an impediment of the use of graphite as negative electrode in lithium-ion cells is the loss of capacity during the first charge/discharge cycle. Yazami et al.<sup>2</sup> showed that lithium can be reversibly inserted into graphite at room temperature<sup>3</sup>. It has been shown that the spacing between the graphite layers increased from 3.35 Å to 3.37 Å upon lithium intercalation<sup>4-6</sup>. This expansion in graphite *d*-spacing may lead to build-up of internal mechanical stresses within graphite layers. Grunes et al.<sup>7</sup> studied distortions of the graphite band structure upon intercalation of alkali metals using electron energy-loss spectroscopy. Christensen and Newman's mathematical model<sup>8</sup> predicted that carbon particle surface was most likely to fracture during de-insertion of lithium-ion. Deshpande et al.<sup>9</sup> developed a model for computing diffusion-induced stresses in electrodes and concluded that the driving force (and probability) of crack formation during de-lithiation and lithiation were different. Results of an experimental study conducted using acoustic emission technique by Ohzuku et al.<sup>10</sup> and Sawai et al.<sup>11</sup> indicated that the rate of fracture of the anode material (MnO<sub>2</sub>) was high during the initial cycle. Using in-situ optical microscopy, Bhattacharya et al.<sup>12</sup> observed occurrence of extensive graphite particle removal during the de-lithiation stage and showed that the potential difference exerted on graphite negative electrode acted as the driving force for graphite surface damage. The damage was arrested when the operating voltage reached a critical value. The magnitude of damage in lithiation stage was much less compared to de-lithiation, which was attributed to the formation of a solid electrolyte layer (SEI).

The structure of the SEI layer is not well known but it was suggested that the SEI film has a mosaic-type structure consisting of polyheteromicrophases<sup>13,14</sup>, where inorganic compounds may predominate in the inner part and organic compounds are usually formed in the outer part<sup>15</sup>. Raman microscopy and AFM studies by Kostecki et al.<sup>16</sup> monitored structural changes of graphite electrodes in lithium-ion cells cycled at room temperature. Degradation events observed at the electrode surface were more pronounced than those observed in the bulk.

Degradation promoted anode surface reactivity with the electrolyte and inorganic decomposition products were found to deposit preferentially at the degraded regions. Zhang et al.<sup>17</sup> suggested that damage in graphite may be due to gas production from electrolyte solution decomposition and subsequent releasing. As proposed by Aurbach et al.<sup>18,19</sup>, ethylene gas could be formed by the decomposition of ethylene carbonate in the electrolyte. Therefore, it is plausible that electrolyte solutions that diffused into cracks inside graphite may decompose and release gases, which might cause an increase of internal pressure causing damage. Focused ion beam microscopy (FIB) has been employed to investigate the formation and evolution of the SEI film on natural graphite spheres<sup>17</sup>, which revealed that initially the thickness range of SEI was 450 - 980 nm when it has a rough, non-uniform morphology, and attained a thickness of approximately 1,600 nm after 24 cycles.

This article focuses on characterization of damage that occurred on graphite electrode surfaces when they were electrochemically cycled between different values of applied potential differences. *In-situ* optical microscopy was used to sequentially observe graphite surface morphology changes. The role of voltage scan rate on the degradation process has been discussed. Cross-sectional microstructures, obtained using FIB milling, were used to investigate the subsurface damage features.

## EXPERIMENTAL

Cylindrical working (negative) electrodes, of 5 mm diameter, made from high purity graphite containing traces of Al, Fe, Mg and Si, were subjected to cyclic voltammetry tests. The electrode surface was prepared using standard metallographic techniques to a final polish using 1200 grit SiC papers and cleaned ultrasonically (to remove the fine graphite particles from the natural cavities present in graphite) using acetone and dried at 100°C for 1 hour. The density of this particular grade of graphite was calculated as 1.6 g/cc.

For in-situ observation of surface degradation of graphite electrodes, a cell with an optical grade quartz glass cover at the top was constructed using chemically modified PTFE having exceptional chemical and permeation resistance. The graphite electrode was placed at the center of the cell. A 99.99% pure lithium wire (containing ~0.01% Na as impurity and a resistivity of 9.446  $\mu\Omega\text{-cm}$  at 20°C) of diameter 3.2 mm, was used as the counter electrode. The reference electrode was also made of a 3.2 mm diameter 99.99% pure lithium wire. The electrolyte solution was formed using a 1 M LiClO<sub>4</sub> (electrolyte salt) in a 1:1 (by vol.) mixture of ethylene carbonate and 1,2-dimethoxy ethane.

The cell components were assembled, and the electrolyte was injected in the cell, inside a glovebox operating in an Argon atmosphere. Cyclic voltammetry tests were performed using a Solartron Modulab Potentiostat/Galvanostat between a base voltage of 0.00 V and different peak voltages of 0.50 V, 1.00 V, 2.00 V and 3.00 V, at scan rates of 500  $\mu\text{V/s}$ , 2 mV/s, 5 mV/s and 10 mV/s. The open-circuit potential of the completed lithium-ion cells was 3.20 V.

Surface morphologies of cycled graphite electrodes were observed using an optical surface profilometer WYKO NT 1100 that utilizes white-light interferometry and a FEI Quanta 200 FEG Scanning Electron Microscope (SEM). Optical profilometer data was collected over a cumulative area of 225×296  $\mu\text{m}^2$  using an average of 5 selected regions on graphite surface. Damaged subsurface microstructures were obtained from cross-sections using a Zeiss NVISION 40 dual beam SEM/FIB. Cross-sectional trenches were milled at specific locations on cycled graphite at an accelerating voltage of 30 kV. Final milling was conducted at low ion-beam currents ranging from 80 - 40 pA.